Solar Cells

DOI: 10.1002/anie.201205007

The Molecular Engineering of Organic Sensitizers for Solar-Cell Applications**

*Jared H. Delcamp, Aswani Yella, Thomas W. Holcombe, Mohammad K. Nazeeruddin, and Michael Grätzel**

Organic materials with attractive electronic and optoelectronic properties for functional device applications are in high demand.[1–6] Organic alternatives to inorganic counterparts are desirable because of the potential to decrease manufacturing costs and realize a more diverse set of devices, including lightweight, efficient low-light, and flexible solar cells. Substantial progress has been made toward functional organic materials for solar-to-electricity conversion.[7,8] Among photovoltaics, dye-sensitized solar-cell (DSC) research has progressed toward becoming a significant contributor to the solar energy conversion market since the seminal work of O'Regan and Grätzel in 1991.[9,10] DSCs are particularly attractive as light-harvesting devices because they allow for judicious control of device properties.[4]

DSCs operate by photoexcitation of a sensitizer (dye) anchored to a semiconductor (such as TiO_2), enabling the transfer of an electron to the semiconductor conduction band followed by regeneration of the dye to the ground-state by a redox shuttle. Metal-based dyes currently yield the highest power conversion efficiencies (PCEs) in DSC devices.[11–16] However, metal-free dyes have recently produced comparably efficient DSCs, often have a much larger molar absorptivity, and may be more cost effective considering the price of precious metals.[17–19] Among organic dyes, the donor–π-bridge–acceptor (D-π-A) structural arrangement is particularly promising.[5] Herein we report the synthesis, characterization, and DSC device performance of an electron-rich heterocycle with the common name ullazine (**1**).

Ullazine is a 16 π-electron nitrogen-containing heterocyclic system that is isoelectronic with pyrene. It was first reportedly synthesized in 1983 to study radical cation and anion persistence (Figure 1).[21,22] An aromatic, 14 π-electron annulene resonance structure consisting of a centralized positive charge upon donation of electron density from the in-plane nitrogen illustrates the potential donating strength as well as electron stabilizing properties of this nitrogen-containing heterocycle (Figure 1, top center). Initial anion/cation stability studies[22] and a computational comparison study to pyrene (see the Supporting Information) suggest that ullazine may be a good candidate for incorporation into π-conjugated materials with optoelectronic applications. Specifically, ullazine possesses 1) a planar π-system to promote strong ICT; 2) both strong donating (push) and (surprisingly) electron-accepting (pull) properties; and 3) multiple substitution sites for molecular engineering.

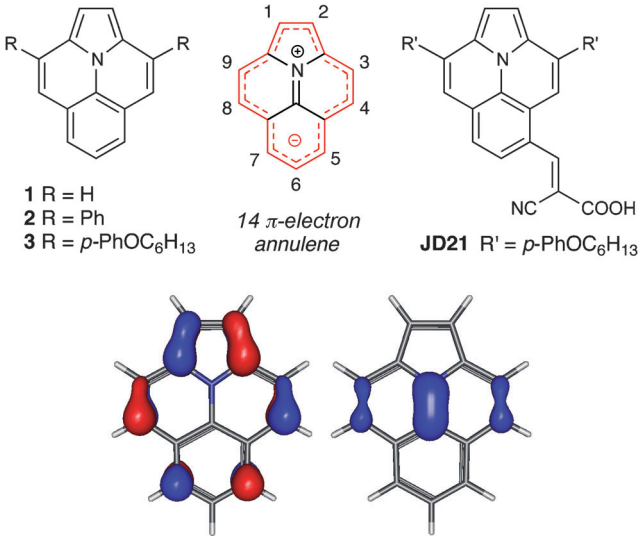

Figure 1. Ullazine structures, with the HOMO (bottom left) and LUMO (bottom right).

DFT calculations of the HOMO and LUMO orbital positions suggest a substantial influence from the positively charged iminium resonance structure (Figure 1). The HOMO of the ullazine heterocycle is largely delocalized around the periphery, with the 6-positions being the only accessible substitution site without a significant HOMO coefficient. The LUMO primarily resides on the central nitrogen and carbon atoms of the iminium motif, with a lesser presence on the 3- and 4-positions of the ullazine periphery. The LUMO position of ullazine is in stark contrast with the LUMO position of the isoelectronic pyrene (Supporting Information, Figure S6).

Substitutions at the 3- and 9-positions of ullazine are known to improve stability, based on the previous studies of Gerson.[22] We envisioned a direct functionalization of the

[*] Dr. J. H. Delcamp, Dr. A. Yella, Dr. T. W. Holcombe, Dr. Md. K. Nazeeruddin, Prof. M. Grätzel
Laboratory for Photonics and Interfaces, Institution of Chemical Sciences and Engineering, School of Basic Sciences
Swiss Federal Institute of Technology, 1015 Lausanne (Switzerland)
E-mail: michael.graetzel@epfl.ch

[**] This work was financially supported by the FP7-Energy-2010-FET project Molesol (contract No. 256617). M.G. thanks the European Research Council (ERC) for an advanced research grant (ARG) to support the Mesolight project. M.K.N. thanks the World Class University program funded by the Ministry of Education, Science and Technology through the National Research Foundation of Korea (R31-2011-000-10035-0), Department of Materials Chemistry, Korea University. A.Y. thanks the Balzan Foundation for partial financial support as part of the 2009 Balzan Prize awarded to M.G.

Supporting information for this article is available on the WWW under http://dx.doi.org/10.1002/anie.201205007.

stabilized ullazine core to maintain a concise synthesis. Installation of late-stage conjugated acceptor/anchor functionality to the ullazine core through electrophilic aromatic substitution (EAS) was examined. Based on the DFT studies, EAS will occur at the 4- and 5-positions of unsubstituted ullazine. Substitution at the 5-position is both preferential to maintain planarity for promotion of a strong ICT and favorable based on the steric influence of substituents at the 3- and 9-positions.

The Balli synthesis of 3,9-diphenyl ullazine (**2**) requires ten steps from present-day, commercially available materials, with an expected 19% overall yield (Scheme 1). This original

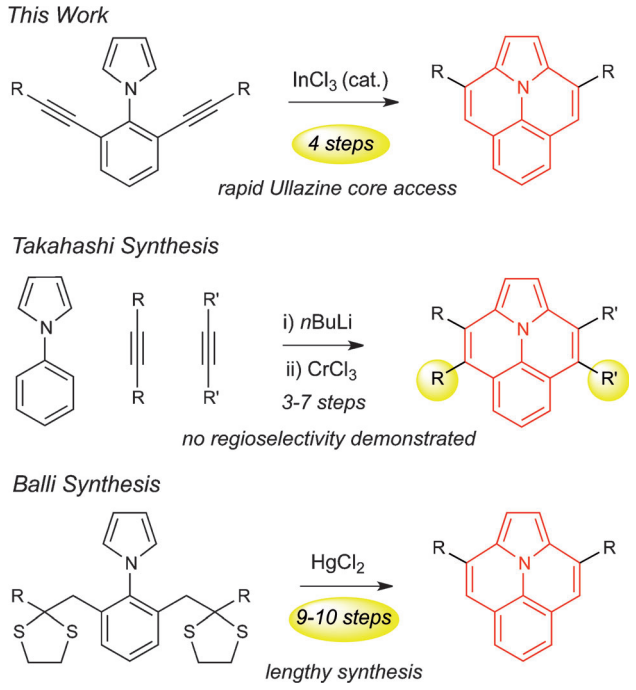

Scheme 1. Key transformations for accessing ullazine heterocycles.

route relies on a lengthy series of oxidation/reduction reactions (two steps) and functional-group manipulations (three steps), which install and remove oxygen and sulfur functionality not present in the final structure. Additionally, as no regioselective reactions to generate the 4,8-unsubstituted ullazine were demonstrated by the Takahashi route (Scheme 1),[23] alternate synthetic routes were examined.

A metal-catalyzed cyclization/hydride shift reaction has been described that can dramatically streamline the synthesis of the desired ullazine structures **2** and **3**. Based on the key transformation described by Fürstner, intermediate **3** could be formed in only four steps with all reactions forming bond connections present in ullazine **3**.[24,25] The synthesis of **3** began with a Paal–Knorr condensation to form the pyrrole intermediate **6** from 2,6-dibromoaniline, followed by a double Sonogashira coupling with alkyne **7** to give pyrrole intermediate **8** in 76% yield (two steps; Supporting Information, Figure S1). Bis(alkyne) **8** was found to undergo a double cyclization/hydride shift reaction in the presence of catalytic $InCl_3$ to give the desired intermediate **3**. The synthesis of the 3,9-bisaryl-substituted ullazine core by a double Fürstner cyclization proceeded in four total steps from commercial starting materials on 5 g scale and in 55% overall yield.

The ground-state oxidation potential ($E_{(S+/S)}$) and excited-state oxidation potential ($E_{(S+/S^*)}$) of ullazine **3** were determined for comparison to a commonly used donor motif in organic electronics, bis(4-hexyloxyphenyl)phenylamine (**4**; Supporting Information, Table 1).[26–28] Ullazine **3** demonstrates a slight decrease (20 mV) in $E_{(S+/S)}$ when compared to **4**, which indicates a similar electron-donating strength. However, **3** shows a large stabilization of $E_{(S+/S^*)}$ (680 mV), as derived from the equation $E_{(S+/S^*)} = E_{(S+/S)} - E_{(0-0)}$ (Table 1). The stabilized $E_{(S+/S^*)}$ may in part result from the resonance contribution of a 14 π-electron aromatic annulene around an electron-accepting iminium core (Figure 1).

Table 1: Optical and electrochemical data.[a]

Compound	λ_{max} [nm][b]	ε [L mol^{-1} cm^{-1}]	$E_{(0\text{-}0)}$ [eV][c]	$E_{(S+/S)}$ [V][d]	$E_{(S+/S^*)}$ [V][e]
Ullazine and triarylamine					
3	393	19400	2.74	0.89	−1.85
4	299	20500	3.44	0.91	−2.53
Ullazine sensitizers					
JD21	582	28000	2.03	1.09	−0.94
JD25	598	33000	1.99	1.03	−0.96
JD26	548, 570[f]	7500[f]	2.06	1.06	−1.00
JD29	598	24000	2.00	1.09	−0.91
JD30	531	12000	2.05	1.09	−0.96
JD32	393, 540[f]	1600[f]	2.08	1.04	−1.04

[a] $E_{(S+/S)}$ and $E_{(S+/S^*)}$ vs. NHE. [b] Measured in CH_2Cl_2. [c] Measured at the intersection of the normalized absorbance and emission spectra. [d] Measured in CH_2Cl_2, 0.1 M Bu_4NPF_6, glassy carbon working electrode, Pt reference electrode, and Pt counter electrode with ferrocene as an internal standard. [e] Calculated from $E_{(S+/S^*)} = (E_{(S+/S)} - E_{(0-0)})$. [f] Shoulder.

EAS was performed on **3** to install a functional handle to the ullazine core for DSC applications. The Villsmeyer–Haack reaction on **3** provided the formylated ullazine intermediate **9** in 81% yield (Supporting Information, Figure S1). The aldehyde **9** then smoothly underwent condensation with cyanoacetic acid to give dye JD21 in 97% yield. The $InCl_3$-based double cyclization route was implemented for the synthesis of five additional dyes that vary the acceptor position or the donor groups on the ullazine core (Scheme 2).

The absorption properties of each of the ullazine-based dyes were examined to better understand the effects of substituents on the ICT band. JD21 has a strong absorbance from 400–625 nm with a λ_{max} at 575 nm and a maximum molar absorbtivity ε of 28000 L mol^{-1} cm^{-1} in dichloromethane (Supporting Information, Figure S11). Dyes JD21, JD25, JD29, and JD30 have a similar absorption maximum and onset. JD29 differs in absorption spectrum shape by a significant increase in the high-energy spectral region. Although the λ_{max} of JD26 is blue-shifted by >40 nm, the λ_{max} peak is significantly broadened and the onset is slightly red-shifted when compared with JD21. JD26 also experiences a signifi-

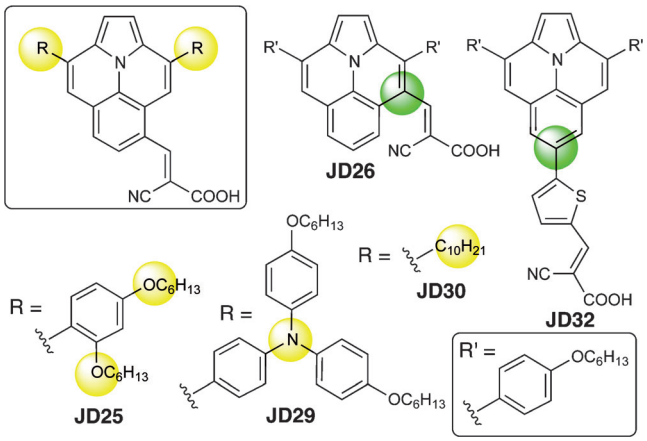

Scheme 2. Ullazine-based dyes for examining the donor and acceptor influence on ICT strength, cation stability, and surface coverage.

cantly depressed molar absorptivity, which indicates the 4-position anchor experiences a loss of planarity. Interestingly, the λ_{max} of JD32, with the anchor in the 6-position of ullazine, blue-shifts by nearly 200 nm compared to JD21. Based on the DFT calculations of the ullazine core, poor electronic communication was expected for 6-substituted ullazine, as a node is observed at this position. Furthermore, the ICT band of JD32 is dramatically decreased to only a slight shoulder ($\varepsilon = 1600\ L\,mol^{-1}\,cm^{-1}$).

Computational studies were performed to examine the influence of an acceptor on the 1-position of ullazine (**10**; Supporting Information, Figure S7). TD-DFT calculations were performed for comparison of dyes JD21, JD26, JD32, and **10**. These studies indicate the largest red shift of the ICT band is observed when placing electron-accepting functionalities at the 4-, 5-, or 6-positions of the ullazine core with the 4- and 5-positions providing the highest oscillator strength (Supporting Information, Figure S8, Table S1). The synthetically challenging dye **10** was not pursued because **10** was the most blue-shifted dye with a lower oscillator strength than the already low-absorbing JD26.

Cyclic voltammetry and absorption/emission spectra for each of the dyes was measured to determine the ground-state oxidation potential ($E_{(S+/S)}$) and HOMO–LUMO transition energy ($E_{(0\text{-}0)}$) values, respectively (Table 1 and Supporting Information). The $E_{(S+/S)}$ values were measured to be within a concise range for all the dyes, from 1.03–1.09 V vs. NHE (Table 1). These values are substantially more positive than the iodide/triiodide redox shuttle, which indicates that the ground-state sensitizer regeneration is energetically favorable for DSC applications.[29] The $E_{(0-0)}$ values were found from the intersection of the absorption and emission spectra for each of the dyes (Supporting Information, Figure S11). The $E_{(S+/S^*)}$ values were calculated to be −0.91 to −1.04 V vs. NHE, which provides the free energy required to transfer an electron from the excited dye to the TiO_2 conduction band.[4] Energetically, a functional DSC device fabricated with the ullazine-based sensitizers, iodide/triiodide redox shuttle and TiO_2 semiconductor is favorable based on the $E_{(S+/S)}$ and $E_{(S+/S^*)}$ values of the dyes.

The application of the ullazine-based dyes as sensitizers for DSC devices was tested with liquid electrolytes (Table 2; Supporting Information, Table S2). Dye JD21 shows a broad

Table 2: Photovoltaic device data with an iodide/triiodide redox shuttle.[a]

Sensitizer	V_{oc} [mV]	J_{sc} [mA cm^{-2}]	FF	PCE [%]
JD21	730	−15.4	0.75	8.4
JD25	807	−11.5	0.72	6.7
JD29	716	−13.3	0.70	6.7
JD30	672	−11.0	0.70	5.2
JD32	553	−3.7	0.78	1.7

[a] For electrolyte compositions, film thickness discussion and N719 comparison, see the Supporting Information. Measured under AM 1.5 with a 6×6 mm^2 black mask.

incident photon-to-electron conversion efficiency (IPCE), from just before 400 nm to approximately 730 nm, with a maximum of 95% at 520 nm (Figure 2). The IPCE range

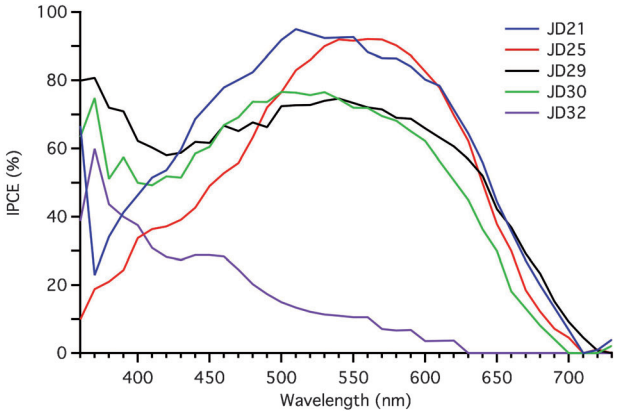

Figure 2. IPCE spectrum for ullazine-based dyes.

is broadened by approximately 75 nm when compared to the solution absorption of JD21 in dichloromethane which may indicate favorable aggregation.[30,31] The integrated current under the IPCE curve is in good agreement with the short-circuit current density (J_{SC}) of −15.4 mA cm^{-2} measured under AM 1.5 conditions. The measured J_{SC} combined with an open-circuit voltage (V_{OC}) of 730 mV and fill factor (FF) of 0.75 gives an excellent power conversion efficiency (PCE or η) of 8.4% according to the equation $\eta = V_{OC}J_{SC}FF/I_{(sun\ intensity)}$. The exceptional performance from low-molecular-weight JD21 (MW = 638 g mol^{-1}, PCE = 8.4%) is exemplified when compared with other low molecular weight dyes.[32] JD21 is a good organic sensitizer candidate for industrial applications based on the concise, scalable (5 g) synthesis (six steps, 43% yield) of JD21, given that several intermediates were well-behaved solids and high performance in DSC devices was achieved. Computationally, electron density contribution from the 3,9-bisalkoxyphenyl substituents of JD21 to the ground-state HOMO is minimal; however, upon cation generation, the alkoxyphenyl substituents contribute substantially to the HOMO orbital delocal-

ization (Supporting Information, Figure S9). Although substituents in the 3- and 9-positions do not dramatically shift the ICT band, they are valuable for controlling morphology and increasing cation stability. The dye cation is a critical intermediate species formed during DSC device operation after electron transfer from the dye to the semiconductor conduction band. Increasing the stability of this charged intermediate and increasing spatial separation of the cation from the semiconductor surface has a direct, positive impact on device performance.[33] DFT calculations with all of the dyes synthesized indicate the LUMO is delocalized on the cyanoacrylic acid acceptor group, which is desirable for efficient charge injection to the TiO_2 conduction band upon dye photoexcitation.

As expected, an acceptor at the 4-position (JD26) proved to be a poor dye for DSC applications, as the dye readily desorbs from the TiO_2 surface, presumably because of the cumbersome steric environment near the anchor. Additionally, placing an acceptor in the 6-position of ullazine dramatically decreased the device short-circuit current, as observed from the IPCE measurements and expected from the UV/Vis data (Supporting Information, Figure S11). Computationally and experimentally (UV, IPCE), the 6-position results in greatly diminished ICT from ullazine to the acceptor.

Dyes JD25, JD29, and JD30 focused on the donor moiety, towards modifying the titanium dioxide surface coverage. Addition of alkyl chains to D-π-A dyes is known to increase DSC device V_{OC} by blocking access to the semiconductor surface, which retards the recombination of electrons in the semiconductor with the redox shuttle.[20] Through the use of two additional hexyloxy chains, the V_{OC} of JD25-based devices was improved by greater than 75 mV in comparison to JD21-based devices. With a V_{OC} of > 800 mV (theoretical max. ca. 850 mV[4]), DSC devices based on the TiO_2 semiconductor, I^-/I_3^- redox shuttle and sensitizer JD25 exhibit minimal loss owing to unfavorable recombination pathways. JD21-based devices have a broader IPCE that extends further into the blue region as expected based on the solution absorption spectrum; however, JD21-based devices demonstrate a larger red-shift of the IPCE spectrum when compared to the solution absorption spectrum than JD25 (75 nm vs. 50 nm). The additional alkoxy substituent of JD25 rotates the phenyl substituent further out of plane with the ullazine π-face and is likely to disrupt any productive aggregate formation.[34]

In conclusion, we have developed a rapid, efficient synthesis of a novel heterocyle for organic electronic applications. The ullazine core is available from simple commercial starting materials in four scalable steps by a double Fürstner cyclization as the key bond-forming reaction. The ullazine core also offers an attractive number of π-conjugated sites for the molecular engineering of ullazine-based functional materials. The unique resonance structure contributions to generate an electron-accepting center and an electron-donating aromatic periphery in part contribute to the remarkable performance exhibited in DSCs with this heterocycle. DSC devices sensitized with metal-free, low-molecular-weight ullazine-based dye JD21 demonstrate an excellent visible absorption spectra resulting in a power conversion efficiency of 8.4%. Owing to the concise, scale-friendly synthesis, and high performance in DSCs, we expect the ullazine core to find widespread use in organic electronic applications with possible industrial applications for the high-efficiency DSC organic dye JD21.

Received: June 26, 2012
Published online: August 24, 2012

Keywords: dyes/pigments · light harvesting · photonics · sensitizers · solar cells

[1] T. M. Figueira-Duarte, K. Müllen, *Chem. Rev.* **2011**, *111*, 7260.
[2] P. M. Beaujuge, J. M. J. Fréchet, *J. Am. Chem. Soc.* **2011**, *133*, 20009.
[3] Y. Shirota, H. Kageyama, *Chem. Rev.* **2007**, *107*, 953.
[4] A. Hagfeldt, G. Boschloo, L. Sun, L. Kloo, H. Pettersson, *Chem. Rev.* **2010**, *110*, 6595.
[5] A. Mishra, M. K. R. Fischer, P. Bäuerle, *Angew. Chem.* **2009**, *121*, 2510; *Angew. Chem. Int. Ed.* **2009**, *48*, 2474.
[6] J. E. Anthony, *Angew. Chem.* **2008**, *120*, 460; *Angew. Chem. Int. Ed.* **2008**, *47*, 452.
[7] Q. Schiermeier, J. Tollefson, T. Scully, A. Witze, O. Morton, *Nature* **2008**, *454*, 816.
[8] L. M. Gonçalves, V. de Zea Bermudez, H. A. Ribeiro, A. M. Mendes, *Energy Environ. Sci.* **2008**, *1*, 655.
[9] B. O'Regan, M. Grätzel, *Nature* **1991**, *353*, 737.
[10] D. Butler, *Nature* **2008**, *454*, 558.
[11] Q. Yu, Y. Wang, Z. Yi, N. Zu, J. Zhang, M. Zhang, P. Wang, *ACS Nano* **2010**, *4*, 6032.
[12] C.-Y. Chen, M. Wang, J.-Y. Li, N. Pootrakulchote, L. Alibabaei, C. Ngoc-le, J.-D. Decoppet, J.-H. Tsai, C. Grätzel, C.-G. Wu, S. M. Zakeeruddin, M. Grätzel, *ACS Nano* **2009**, *3*, 3103.
[13] Y. Chiba, A. Islam, Y. Watanabe, R. Komiya, N. Koide, L. Han, *Jpn. J. Appl. Phys.* **2006**, *45*, L638.
[14] M. K. Nazeeruddin, F. De Angelis, S. Fantacci, A. Selloni, G. Viscardi, P. Liska, S. Ito, B. Takeru, M. Grätzel, *J. Am. Chem. Soc.* **2005**, *127*, 16835.
[15] A. Yella, H.-W. Lee, H. N. Tsao, C. Yi, A. K. Chandiran, M. K. Nazeeruddin, E. W.-G. Diau, C.-Y. Yeh, S. M. Zakeeruddin, M. Grätzel, *Science* **2011**, *334*, 629.
[16] T. Bessho, S. M. Zakeeruddin, C.-Y. Yeh, E. W.-G. Diau, M. Grätzel, *Angew. Chem.* **2010**, *122*, 6796; *Angew. Chem. Int. Ed.* **2010**, *49*, 6646.
[17] H. N. Tsao, C. Yi, T. Moehl, J.-H. Yum, S. M. Zakeeruddin, M. K. Nazeeruddin, M. Grätzel, *ChemSusChem* **2011**, *4*, 591.
[18] Y. Bai, J. Zhang, D. Zhou, Y. Wang, M. Zhang, P. Wang, *J. Am. Chem. Soc.* **2011**, *133*, 11442.
[19] W. Zeng, Y. Cao, Y. Bai, Y. Wang, Y. Shi, M. Zhang, F. Wang, C. Pan, P. Wang, *Chem. Mater.* **2010**, *22*, 1915.
[20] S. Ito, H. Miura, S. Uchida, M. Takata, K. Sumioka, P. Liska, P. Comte, P. Péchy, M. Grätzel, *Chem. Commun.* **2008**, 5194.
[21] H. Balli, M. Zeller, *Helv. Chim. Acta* **1983**, *66*, 2135.
[22] F. Gerson, A. Metzger, *Helv. Chim. Acta* **1983**, *66*, 2031.
[23] K. Kanno, Y. Liu, A. Iesato, K. Nakajima, T. Takahashi, *Org. Lett.* **2005**, *7*, 5453.
[24] V. Mamane, P. Hannen, A. Fürstner, *Chem. Eur. J.* **2004**, *10*, 4556.
[25] A. Fürstner, V. Mamane, *J. Org. Chem.* **2002**, *67*, 6264.
[26] R. Li, J. Liu, N. Cai, M. Zhang, P. Wang, *J. Phys. Chem. B* **2010**, *114*, 4461.
[27] N. G. Connelly, W. E. Geiger, *Chem. Rev.* **1996**, *96*, 877.
[28] R. C. Wheast, *Handbook of Physics and Chemistry*, 63rd ed., CRC, Boca Raton, FL, **1982**.
[29] G. Boschloo, A. Hagfeldt, *Acc. Chem. Res.* **2009**, *42*, 1819.

[30] D. Kuang, S. Uchida, R. Humphry-Baker, S. M. Zakeeruddin, M. Grätzel, *Angew. Chem.* **2008**, *120*, 1949; *Angew. Chem. Int. Ed.* **2008**, *47*, 1923.
[31] T. Horiuchi, H. Miura, S. Uchida, *J. Photochem. Photobiol. A* **2004**, *164*, 29.
[32] C. Teng, X. Yang, S. Li, M. Cheng, A. Hagfeldt, L. Wu, L. Sun, *Chem. Eur. J.* **2010**, *16*, 13127.
[33] Y. Liang, B. Peng, J. Chen, *J. Phys. Chem. C* **2010**, *114*, 10992.
[34] In agreement with a bulkier aryl substituent, dye-loading studies indicate a significantly lower dye adsorption onto the TiO_2 surface for JD25 when compared to JD21 (ca. 30% lower). The dye loading trend follows the same trend as substituent bulk at the 3- and 9-positions of ullazine (SI, Table S3).

